RSC Advances

COMMUNICATION

View Article Online
View Journal | View Issue

Self-assembly of Cu(II) with amyloid β_{19-20} peptide: relevant to Alzheimer's disease†

Cite this: *RSC Adv.*, 2014, **4**, 21840

Xiaofang Shen,* Xiaorong Deng and Yuehong Pang

Received 28th March 2014
Accepted 6th May 2014

DOI: 10.1039/c4ra02758b

www.rsc.org/advances

Amyloid-β (Aβ) peptide $A\beta_{19-20}$ tends to self-assemble into well-ordered tubular structures under physiological conditions, while in the presence of equimolar Cu(II), they assembled into homogeneous microvesicles; a chelator can competitively bind to Cu(II) from the Cu(II)–$A\beta_{19-20}$ complex, resulting in reforming of the peptide tubular structure.

Alzheimer's Disease (AD) is an age-related neurodegenerative disorder characterized by a progressive loss of memory and the deterioration of higher cognitive functions.[1] More than 26 million people worldwide are afflicted by AD. However, no drugs or therapeutics have thus far been developed to treat AD.[2] The self-assembly of amyloid-β (Aβ) peptides into highly ordered amyloid fibril structures represents one of the pathological hallmarks of AD.[3] Under normal conditions, about 90% of secreted Aβ peptides are $A\beta_{1-40}$, species that are highly fibrillogenic and deposited early in individuals with AD.[4] The central seven-residue segment $A\beta_{16-22}$ is thought to be crucial for amyloid fibril formation. While the forepost of such sequences in the full-length peptide do not have that propensity.[5] Furthermore, the amyloid fibril formation of other short beta peptide fragments, such as $A\beta_{1-28}$,[6] $A\beta_{11-17}$,[7] $A\beta_{16-20}$,[8] $A\beta_{16-22}$,[9] $A\beta_{25-35}$,[10] $A\beta_{31-35}$ (ref. 11) and $A\beta_{39-42}$ (ref. 12) are also reported. Short peptides serve as an excellent model system for exploring amyloid fibrils formation in particular and biological self-assembly processes in general.[13]

Since its discovery as a core recognition motif of the Alzheimer's Aβ peptide, $A\beta_{19-20}$ (diphenylalanine, Phe–Phe) has increasingly become the subject of intense investigation in the fields of both medicine and nanotechnology.[14] It has been demonstrated that $A\beta_{19-20}$ tends to self-assemble into well-ordered nanotubes. The formed tubular structures may share some structural properties with the amyloid fibrils as they have similar vibrational spectrum and birefringence as compared to the fibrils.[15] This indicates that the dipeptide aromatic motifs contain all the molecular information needed to form well-ordered-supramolecular structures at the nano-scale. One striking property of the peptide nanotubes is their remarkable rigidity, with a high Young's modulus of 19–27 GPa using two independent techniques.[16] Scientists try to find out why the peptide nanostructures are so rigid.[17] However, little is known about the forces underlying their stability and relationship with the AD. The π–π stacking interactions may accelerate amyloid fibril formation by providing geometrical restrictions that promote directionality and orientation of the growing fibril, together with energetic contributions from the stacking itself.[18] Indeed, replacement of the phenylalanine residues at the C terminus of $A\beta_{1-42}$ by hydrophobic residues resulted in somewhat slower aggregation, while a mutant variant containing four phenylalanine residues at the C terminus of $A\beta_{1-42}$ displayed faster amyloidogenesis.[19]

In an aging brain, metal ions might have a relevant role in the development and progression of the AD disease.[20] The disordering process associated with Aβ aggregation of AD is greatly influenced by the metal ions (*i.e.* Cu, Al, Fe and Zn). The metals are found in both the core and rim of the AD senile plaques. Analysis of the autopsy of AD patients shows abnormally high levels of Cu (~393 μM) present in the senile plaques; the normal cerebral extracellular concentration is 0.2–1.7 μM.[21] The vitro studies also showed that Cu(II) would influence the formation of amyloid fibrils.[20c,22] Cu(II) has been proposed to play a central role in the amyloid cascade process linked to the development of AD. Involvement in both the Aβ aggregation process and reactive oxygen species production has been considered. Researchers have accordingly put forth the "metals hypothesis" of AD, which postulates that compounds designed to inhibit Cu(II)/Aβ interactions and redistribute Cu(II) may offer therapeutic potential for treating AD.[23]

The involvement of Cu(II) with Aβ in AD and the potential development of metal chelating therapy indicate the

State Key Laboratory of Food Science and Technology, School of Food Science and Technology, Jiangnan University, Wuxi, Jiangsu 214122, P.R. China. E-mail: xfshen@jiangnan.edu.cn

† Electronic supplementary information (ESI) available. See DOI: 10.1039/c4ra02758b

importance of elucidating the fundamental mechanisms of Cu(II) effects on short peptide model $A\beta_{19-20}$. Herein, we investigate the Cu(II) ion effects on self-assembly of $A\beta_{19-20}$ peptide and the ability of ethylene diamine tetraacetic acid (EDTA) to compete chelating Cu(II) and then recover the structure of $A\beta_{19-20}$ peptide (Fig. 1A). Actually, we observed the visual change in solutions at the beginning. The addition of Cu(II) to $A\beta_{19-20}$ made the solution appear dark blue. When equimolar EDTA was added to the above mixed solution, the color of the solution became greenish blue, which was consistent with that of Cu(II) with EDTA (Fig. 1B).

Fig. 2 shows the effect of Cu(II) on the self-assembled $A\beta_{19-20}$ tubes aggregates overnight. We could observe the $A\beta_{19-20}$ peptide formed tubes on the solid substrate (Fig. 2 A and C), as reported previously by Gazit group.[14a] The average diameter of the tubes was about 1.0–2.5 μm with a long persistence length, ranging from approximately 100 μm to millimeter. However, in the presence of Cu(II) as molecule ratio to $A\beta_{19-20}$ is 1 : 1, we could not observe tubular structure (Fig. 2B and D). Instead, abundant uniform microvesicles with an average diameter about 0.8–5.0 μm were observed. The transition from tubular structures to dense microvesicles evident from the scanning electron microscopy (SEM) images illustrate that Cu(II) inhibited original peptide tube assembly and formed a new structure.

Cu(II) induced π–π stacking changes of $A\beta_{19-20}$ peptide: We attribute the visual changes in solution and rearrangement of the structures to the π–π interactions of the aromatic rings on phenylalanine. $A\beta_{19-20}$ peptide features aromatic moieties which play a key role in the fibril self-assembly process and drive a well-ordered stacking of aromatic rings by π–π interactions.[14a,e] The UV-vis spectra of various molar ratio of Cu(II) to $A\beta_{19-20}$: 0 : 1, 1 : 4, 1 : 2, 1 : 1 and 2 : 1 in pH 7.4 Tris–HCl buffer

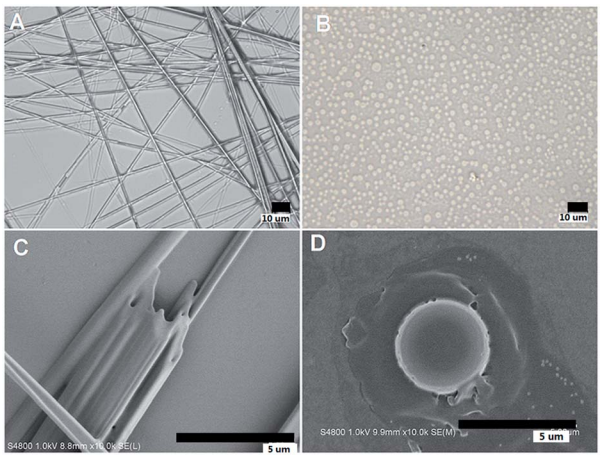

Fig. 2 (A) Self-assembled structures of $A\beta_{19-20}$, (B) 1 : 1 molar ratio of Cu(II) to $A\beta_{19-20}$. (C) and (D) are SEM enlarged images of (A) and (B), respectively. Scale bar: (A) and (B) are 10 μm, (C) and (D) are 5 μm.

are shown in Fig. 3. The absorption peak of $A\beta_{19-20}$ is at 258 nm. It is known that the absorption is attribute to benzene ring characteristic absorption band, which corresponds to the π–π* transition and the vibration of phenyl rings. The addition of the Cu(II) noticeably increased the absorption of $A\beta_{19-20}$ peptide (Fig. 3A). The maximum response was observed when molar ratio of Cu(II) to $A\beta_{19-20}$ reached 1 : 1. The result shows that Cu(II) interacted with $A\beta_{19-20}$ peptide and, to some extent, influenced the vibration of $A\beta_{19-20}$ phenyl rings.

Further evidence of the involvement of aromatic interactions with Cu(II) was provided by fluorescence spectra, which is the crucial to the phenylalanine dipeptide assembly. Fig. 3B shows the fluorescence titration spectra of $A\beta_{19-20}$ peptide with

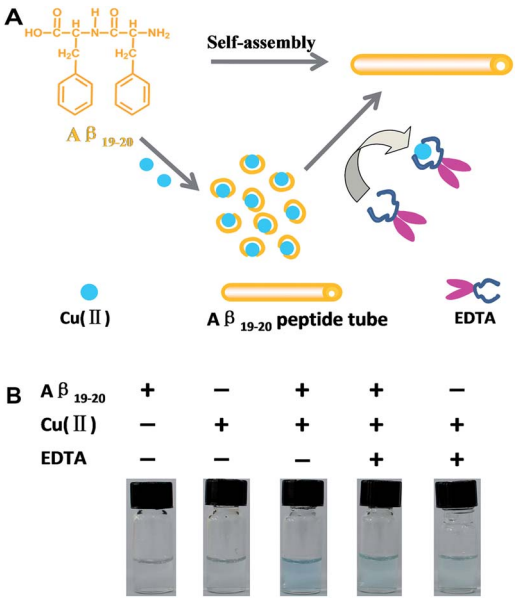

Fig. 1 Schematic representation of (A), $A\beta_{19-20}$ peptide assembly with Cu(II) ions and then EDTA competes to chelate Cu(II), meanwhile (B) the visible change in solutions.

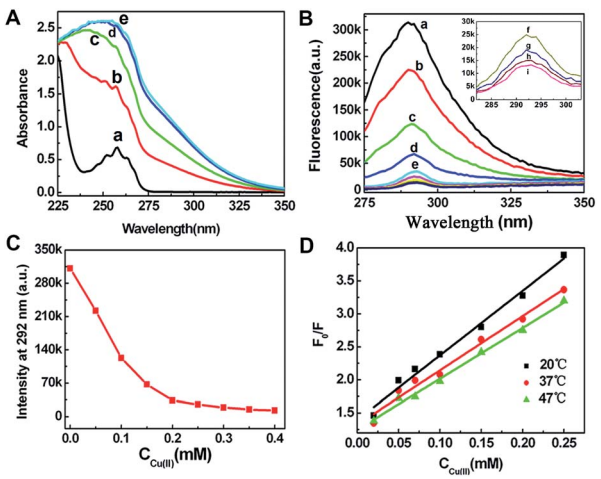

Fig. 3 (A) UV-vis spectra of $A\beta_{19-20}$ at 258 nm with various molar ratio of Cu(II) to $A\beta_{19-20}$. From a to e: 0 : 1, 1 : 4, 1 : 2, 1 : 1 and 2 : 1. (B) Fluorescence titration spectra with different molar ratio of Cu(II) to $A\beta_{19-20}$. From (a) to (i): 0 : 1, 1 : 4, 1 : 2, 1 : 1.3, 1 : 1, 1.25 : 1, 1.5 : 1, 1.75 : 1 and 2 : 1. Inset is enlarged from (f) to (i). (C) Nonlinear fitting curve of $A\beta_{19-20}$ peptide binding to Cu(II). (D) The Stern–Volmer plots for the quenching of fluorescence by Cu(II) at 20, 37 and 47 °C.

different concentrations of Cu(II) solution. $A\beta_{19-20}$ possesses two phenylalanine residues that emitted fluorescence with the maximum at 292 nm upon excitation at 265 nm, which was belonging to the π–π stacking interactions.[24] The decrease in the fluorescence intensity was the most marked change with the successive addition of Cu(II), indicating that the fluorescence of $A\beta_{19-20}$ was quenched. The curve has a tendency towards invariability at Cu(II)/$A\beta_{19-20}$ molar ratio of 1 : 1(Fig. 3C), indicating the Cu(II) influenced the π–π stacking of $A\beta_{19-20}$.

Intrinsic peptide fluorescence is a useful and sensitive tool to study variations in a peptide conformation and its interactions with other molecules.[7] To understand the interaction stoichiometry of $A\beta_{19-20}$ peptide with Cu(II) ions, fluorescence titration method was used and the nonlinear fitting curve of $A\beta_{19-20}$ peptide binding to Cu(II) (ESI†). The fluorescence titration data processing can be described as follows:[22b,25] Assuming a protein-to-ligand binding reaction ($P + nL \leftrightarrow PL_n$), the fraction of bound ligand (γ) can be related to the equilibrium dissociation constant (K_d), as shown in eqn (1).

$$K_d = \frac{\gamma}{(1-\gamma)(L_t - n\gamma P_t)} \quad (1)$$

Where P_t and L_t are the concentration of $A\beta_{19-20}$ and Cu(II), respectively. γ is the fraction of the observed fluorescence signal changes and the maximum fluorescence signal changes, as shown in eqn (2).

$$\gamma = \frac{\Delta F}{\Delta F_{max}} \quad (2)$$

Combining eqn (1) and (2) yields (3):

$$\frac{\Delta F}{\Delta F_{max}} = \frac{(K_d + L_t + nP_t) - \sqrt{(K_d + L_t + nP_t)^2 - 4nP_tL_t}}{2nP_t} \quad (3)$$

According to eqn (3), K_d can be obtained. The fractions of $A\beta_{19-20}$ bound with Cu(II) were plotted against the Cu(II) concentration. The data could be fitted to a single ligand binding with the equilibrium dissociation constant, $K_d = 4.24$ μM, suggesting a high affinity of $A\beta_{19-20}$ peptide with Cu(II).

Cu(II) ion caused $A\beta_{19-20}$ peptide endogenous fluorescence quenching regularly, but did not influence the excited fluorescence molecular state, thus altering the absorption spectrum. This may be due to Cu(II) associated with $A\beta_{19-20}$ and complex form, resulting in peptide fluorescence static quenching. Static quenching and dynamic quenching vary temperature. The quenching rate constants decrease with increasing temperature for static quenching, but the reverse effect is observed for the case of dynamic quenching.[25] To further characterize the quenching mold, a possible quenching mechanism was evident from the Stern–Volmer curves of $A\beta_{19-20}$ with Cu(II) at different temperatures (20, 37 and 47 °C) as shown in Fig. 3D. The Stern–Volmer plots were linear, the slopes of which decreased with increasing temperature. This indicated the occurrence of a static quenching interaction between $A\beta_{19-20}$ and Cu(II). Quenching data were then fit into the Stern–Volmer eqn (4).

$$\frac{F_0}{F} = 1 + K_{SV}[Q] \quad (4)$$

Where F_0 and F are the fluorescence intensity in the absence and in the presence of quencher $[Q]$ respectively and K_{SV} is the Stern–Volmer quenching constant. K_{SV} was the slope of the linear regression of the Stern–Volmer relationship [eqn (4)] and it was 9.8 mM^{-1} (20 °C), 8.2 mM^{-1} (37 °C) and 7.7 mM^{-1} (47 °C). K_{SV} decreased with the increase of temperature, which indicated that lower temperature would ease $A\beta_{19-20}$ peptide quenching and accessibility to Cu(II).

To demonstrate that Cu(II) influenced and mediated the assembly of $A\beta_{19-20}$ peptides, we performed chelation competition experiments with chelator. EDTA exerting an antagonizing effect on the Cu(II)-induced changes of the intrinsic fluorescence of $A\beta_{19-20}$ peptide. The intrinsic fluorescence of $A\beta_{19-20}$ peptide was gradually recovered and reached maximum at 48 h (ESI†). Morphological changes also reveal the competitive chelation of the chelator to Cu(II) from $A\beta_{19-20}$ (Fig. 4). Co-existed 3.2 mM $A\beta_{19-20}$ peptide and equimolar Cu(II) self-assembled into homogeneous microvesicles (Fig. 4A). Interestingly, when the equimolar chelating agent EDTA was injected into Cu(II) and $A\beta_{19-20}$ peptide mixed solution, enabling it to chelate Cu(II) from Cu(II)–$A\beta_{19-20}$ complex. As a result, microvesicles disappeared and the peptide tubular structures were obtained (Fig. 4B).

Cu(II) ions interact with $A\beta_{19-20}$ peptide and form Cu(II)–$A\beta_{19-20}$ complex, which influenced π–π stacking of $A\beta_{19-20}$ peptide and induced its morphology from dense tubes to an homogeneous microvesicles. Chelator can completely chelate Cu(II) from Cu(II)–$A\beta_{19-20}$ complex and reform $A\beta_{19-20}$ peptide tubular structure. These results facilitate the understanding of the clinically related Cu(II) ions with Aβ in AD and provide a rationalized mechanism for fibrils formation. However, due to the complex etiology of AD, a simple interaction model currently is not possible for fully understanding the disease. On the one hand, high-resolution structural studies of amyloid fibrils have made huge progress in recent years, such as utilizing a variety of $^{13}C/^{15}N$-labeling strategies and combined with multidimensional magic angle spinning (MAS) NMR techniques,[26] and the combination of electron paramagnetic resonance (EPR) spectroscopy with isotopic labelling.[27] These techniques can unambiguously determine the Cu^{2+}/Aβ coordination to provide credible new insights into the assembly. On the other hand, development of novel classes of potential

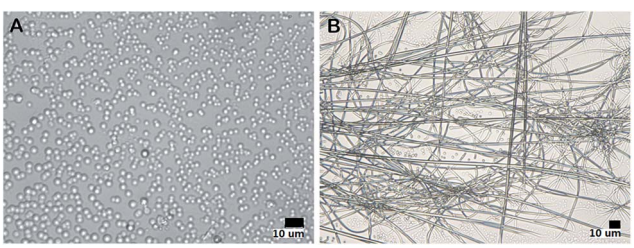

Fig. 4 (A) Microvesicles self-assembled by $A\beta_{19-20}$ peptide with equimolar Cu(II). (B) Tubular structures of $A\beta_{19-20}$ reformed in the presence of EDTA. Scale bar is 10 μm.

therapeutics using the tools of coordination chemistry to create synthetic ligands for competing metal ions with Aβ, one can hope these will actually derail these diseases in the future.

This work was supported by the National Natural Science Foundation of China (21005032) and the Natural Science Foundation of Jiangsu Province (BK2012107).

Notes and references

1 (*a*) N. C. Berchtold and C. W. Cotman, *Neurobiol. Aging*, 1998, **19**, 173–189; (*b*) R. D. Terry and R. Katzman, *Ann. Neurol.*, 1983, **14**, 497–506.
2 (*a*) D. Kim, N. H. Kim and S. H. Kim, *Angew. Chem., Int. Ed.*, 2013, **52**, 1139–1142; (*b*) M. A. Telpoukhovskaia and C. Orvig, *Chem. Soc. Rev.*, 2013, **42**, 1836–1846.
3 (*a*) M. P. Murphy and H. LeVine, *J. Alzheimer's Dis.*, 2010, **19**, 311–323; (*b*) C. Haass and D. J. Selkoe, *Nat. Rev. Mol. Cell Biol.*, 2007, **8**, 101–112; (*c*) W. Bondareff, *J. Alzheimer's Dis.*, 2013, **35**, 1–6; (*d*) I. W. Hamley, *Chem. Rev.*, 2012, **112**, 5147–5192.
4 S. Kar, S. P. M. Slowikowski, D. Westaway and H. T. J. Mount, *J. Neuropsychiatry Clin. Neurosci.*, 2004, **29**, 427–441.
5 C. SivakamaSundari, S. Rukmani and R. Nagaraj, *J. Pept. Sci.*, 2012, **18**, 122–128.
6 T. Wasiak, M. Ionov, K. Nieznanski, H. Nieznanska, O. Klementieva, M. Granell, J. Cladera, J.-P. Majoral, A. M. Caminade and B. Klajnert, *Mol. Pharmaceutics*, 2012, **9**, 458–469.
7 C. He, Y. Han, Y. Fan, M. Deng and Y. Wang, *Langmuir*, 2012, **28**, 3391–3396.
8 S. Dehn, V. Castelletto, I. W. Hamley and S. Perrier, *Biomacromolecules*, 2012, **13**, 2739–2747.
9 N. Chaudhary and R. Nagaraj, *J. Pept. Sci.*, 2011, **17**, 115–123.
10 M. Naldi, J. Fiori, M. Pistolozzi, A. F. Drake, C. Bertucci, R. Wu, K. Mlynarczyk, S. Filipek, A. De Simone and V. Andrisano, *ACS Chem. Neurosci.*, 2012, **3**, 952–962.
11 Y. Kuroki, Y. Sasaki, D. Kamei, Y. Akitake, M. Takahashi, S. Uematsu, S. Akira, Y. Nakatani, I. Kudo and S. Hara, *Biochem. Biophys. Res. Commun.*, 2012, **424**, 409–413.
12 M. M. Gessel, C. Wu, H. Li, G. Bitan, J.-E. Shea and M. T. Bowers, *Biochemistry*, 2012, **51**, 108–117.
13 M. Reches and E. Gazit, *Curr. Nanosci.*, 2006, **2**, 105–111.
14 (*a*) M. Reches and E. Gazit, *Science*, 2003, **300**, 625–627; (*b*) E. Gazit, *Chem. Soc. Rev.*, 2007, **36**, 1263–1269; (*c*) X. Yan, P. Zhu and J. Li, *Chem. Soc. Rev.*, 2010, **39**, 1877–1890; (*d*) I. Cherny and E. Gazit, *Angew. Chem., Int. Ed.*, 2008, **47**, 4062–4069; (*e*) M. Reches and E. Gazit, *Nat. Nanotechnol.*, 2006, **1**, 195–200.
15 E. Gazit, *Prion*, 2007, **1**, 32–35.
16 (*a*) X. H. Yan, P. L. Zhu and J. B. Li, *Chem. Soc. Rev.*, 2010, **39**, 1877–1890; (*b*) N. Kol, L. A. Abramovich, D. Barlam, R. Z. Shneck, E. Gazit and I. Rousso, *Nano Lett.*, 2005, **5**, 1343–1346; (*c*) L. Niu, X. Chen, S. Allen and S. J. B. Tendler, *Langmuir*, 2007, **23**, 7443–7446.
17 I. Azuri, L. Adler-Abramovich, E. Gazit, O. Hod and L. Kronik, *J. Am. Chem. Soc.*, 2014, **136**, 963–969.
18 I. Cherny and E. Gazit, *Angew. Chem., Int. Ed.*, 2008, **47**, 4062–4069.
19 W. Kim and M. H. Hecht, *Proc. Natl. Acad. Sci. U. S. A.*, 2006, **103**, 15824–15829.
20 (*a*) P. Zatta, D. Drago, S. Bolognin and S. L. Sensi, *Trends Pharmacol. Sci.*, 2009, **30**, 346–355; (*b*) M. A. Telpoukhovskaia and C. Orvig, *Chem. Soc. Rev.*, 2013, **42**, 1836–1846; (*c*) F. Hane, G. Tran, S. J. Attwood and Z. Leonenko, *PLoS One*, 2013, **8**, e59005; (*d*) D. Pramanik, C. Ghosh, S. Mukherjee and S. G. Dey, *Coord. Chem. Rev.*, 2013, **257**, 81–92.
21 (*a*) C. Bouras, P. Giannakopoulos, P. F. Good, A. Hsu, P. R. Hof and D. P. Perl, *Eur. Neurol.*, 1997, **38**, 53–58; (*b*) M. A. Lovell, J. D. Robertson, W. J. Teesdale, J. L. Campbell and W. R. Markesbery, *J. Neurol. Sci.*, 1998, **158**, 47–52.
22 (*a*) S. Bolognin, L. Messori, D. Drago, C. Gabbiani, L. Cendron and P. Zatta, *Int. J. Biochem. Cell Biol.*, 2011, **43**, 877–885; (*b*) W. T. Chen, Y. H. Liao, H. M. Yu, I. H. Cheng and Y. R. Chen, *J. Biol. Chem.*, 2011, **286**, 9646–9656; (*c*) B. Alies, E. Renaglia, M. Rozga, W. Bal, P. Faller and C. Hureau, *Anal. Chem.*, 2013, **85**, 1501–1508.
23 (*a*) Y. Jiao and P. Yang, *J. Phys. Chem. B*, 2007, **111**, 7646–7655; (*b*) S. C. Drew, C. J. Noble, C. L. Masters, G. R. Hanson and K. J. Barnham, *J. Am. Chem. Soc.*, 2009, **131**, 1195–1207; (*c*) C. Hureau, *Coord. Chem. Rev.*, 2012, **256**, 2164–2174; (*d*) S. C. Drew and K. J. Barnham, *Acc. Chem. Res.*, 2011, **44**, 1146–1155; (*e*) H. A. Feaga, R. C. Maduka, M. N. Foster and V. A. Szalai, *Inorg. Chem.*, 2011, **50**, 1614–1618.
24 P. Zhu, X. Yan, Y. Su, Y. Yang and J. Li, *Chem.–Eur. J.*, 2010, **16**, 3176–3183.
25 Y. R. Chen and A. C. Clark, *Protein Sci.*, 2004, **13**, 2196–2206.
26 Y. C. Su, C. J. Sarell, M. T. Eddy, G. T. Debelouchina, L. B. Andreas, C. L. Pashley, S. E. Radford and R. G. Griffin, *J. Am. Chem. Soc.*, 2014, **136**, 6313–6325.
27 S. C. Drew and K. J. Barnham, *Acc. Chem. Res.*, 2011, **44**, 1146–1155.